Photodegradation of Rhodamine B catalyzed by ZnO pellets

T. M. O. Ruellas[1]*, G. H. S. Domingos[1], L. O. O. Peçanha[1], S. C. Maestrelli[1], T. R. Giraldi[1]
[1]Universidade Federal de Alfenas, Instituto de Ciência e Tecnologia, Rod. José Aurélio Vilela 11999, 37715-400, Poços de Caldas, MG, Brazil

Abstract

This paper describes the development of ZnO semiconductors applied as photocatalysts for the degradation of water contaminants, with the shape of ceramic pellets thick enough to maintain their structures, prepared by slip casting and sintering. The samples presented porosities around 40% and densities around 3.4 g/cm^3, which represented about 61% of the theoretical density of ZnO. After obtaining the ceramic samples, the degradation of Rhodamine B dye by photocatalysis was evaluated in six cycles of degradation. After the cycles, changes in the surface of the samples were verified, possibly due to leaching during photocatalysis since they presented mean grain sizes of 0.61 μm before and 0.36 μm after the photocatalysis. The ceramic ZnO samples were able to satisfactorily degrade Rhodamine B for several cycles, resulting in successful reuse of photocatalysts and increased facility of removing the photocatalysts from the medium after degradation compared to powders in suspensions.
Keywords: slip casting, semiconductors, photocatalysis, Rhodamine B, ZnO.

INTRODUCTION

The proper management and use of water are one of the main focuses when it comes to achieving sustainable development in modern society. Several processes that use water generate several types of highly toxic effluents or with high microbial and bacterial activity, which makes them unsuitable for reuse in agricultural activities and for human use. Thus, in the last decades, the recycling of water has become one of the most focused subjects in several researches [1-5]. One of the examples of industrial activity that contributes to the generation of large quantities of contaminated liquid effluents is textile production. The wastes generated by this activity are often contaminated with organic dyes, since they are one of the main components of the dyes used in the textile industries. Thus, recently, catalyzed processes that use solar energy to promote catalysis of organic dyes have been studied [6, 7]. Several methods are used in the treatment of wastewater, mainly physicochemical, biological and chemical. For the removal of dyes from textile effluents, physicochemical methods use treatments such as adsorption, coagulation, filtration, and flocculation, which are effective in discoloration. However, they present the disadvantages of producing sludge, losses and high cost in adsorbent regeneration and, in the case of membranes which do not produce sludge, high cost and productivity reduction over time due to membrane obstruction are negative factors [8, 9]. The treatment of these contaminants, in general, is highly complex. In many cases, the desired efficiency for proper treatment is only achieved by combining two or more processes. Among the most important processes are the advanced oxidative processes (AOPs), which involve the generation and consumption of highly oxidizing and non-selective species, especially the hydroxyl radical (•OH) and, in some cases, the atomic oxygen [O(1D)] [10].

Chemical processes such as ozonation and oxidation through hypochlorite ion, as well as the AOPs, provide rapid degradation of the dyes [8]. AOPs are environmentally correct methods that generate highly reactive species, such as the hydroxyl radical (OH•), whose standard reduction potential is much higher than those of common oxidants, reacting with organic molecules rapidly and in a non-selective way, either by addition to the double bond or by abstraction of the hydrogen atom in aliphatic organic molecules. In many cases, the action of intermediates such as the hydroxyl radical is the only viable way of oxidizing an organic compound to carbon dioxide and water. The hydroxyl radical can be used successfully in the degradation of organic pollutants [11, 12]. Photocatalysis is one of these AOPs used in dye degradation. According to IUPAC (International Union of Pure and Applied Chemistry), photocatalysis consists of the catalytic reaction in which there is the absorption of ultraviolet, visible light, or infrared radiation by the catalyst, usually a semiconductor [13]. Zinc oxide (ZnO) is one of the most studied semiconductors due to its favorable characteristics, such as non-toxicity, good photocatalytic efficiency, good detection behavior, among others [14]. The use of photocatalysts in the form of powder, although common due to the high surface area, presents several difficulties that affect its applicability in large scale. One is the withdrawal complexity, which is usually a costly process due to the size of the particles, generally smaller than 1 μm [15, 16]. The suspended particles also tend to aggregate, which decreases their efficiency, especially in cases where the concentration of suspended particles is high. In addition, the use of suspensions is hampered in continuous flow systems and often the photocatalyst is lost [15-18]. One of the alternatives is the use of these materials

**thamararuellas@gmail.com*
https://orcid.org/0000-0002-7192-6068

in the immobilized form, since they can be removed in a much simpler way, besides the possibility of reuse, being an industrially desired technique [16, 17]. Therefore, the immobilized pellets must have high porosity in addition to high adsorption capacity, aiming a greater surface area and a greater interaction with the organic pollutant [15]. For this purpose, this paper aimed to obtain pellets as the immobilization form using ZnO by slip casting. There are other papers in the literature that have obtained ZnO in other forms of immobilization, such as thin films [19-22].

In order to obtain an immobilized pellet, slip casting was used. This ceramic forming process is simple, old and can be used to produce traditional or advanced ceramics in the most varied shapes. The process consists of the preparation of a powder suspension, usually in water, which is then poured into a porous plaster mold [23]. The porosity of the plaster molds is one of the determining factors of the properties and structure of the pellets obtained through the process of slip casting [24]. Obtaining green bodies with homogeneous microstructures is desired, since it affects the behavior of the ceramic in the sintering process and in its final properties [25]. Plaster is an easy-to-mold, fragile, porous, and low-cost material [26, 27] being the most commonly used material in the production of molds. After the forming process, it is necessary to dry the pellet. The purpose of drying is to remove excess water, a process of heat and mass transfers [28, 29] that allows the physical and chemical properties of the final pellet to be controlled. This step is essential due to the high humidity and temperature gradients that exist inside the pellet and, consequently, thermal and water stresses resulting from these gradients, which directly affect the produced ceramic, causing irreversible defects and increased costs [30-32]. The sintering process, subsequent to drying, is responsible for conferring the desired final characteristics of the pellet. This term is used when the heating temperature is between 50% and 75% of the melting temperature of the material [33]. During the heat treatment, changes in size and shape of the grains, as well as in the pores, may occur. In the solid-state sintering, which is this paper's case, the particles are bonded through atomic diffusion forming grains, and the beginning of the matter transport between two grains can be called neck formation. Normally, during sintering, the porosity of the pellet decreases, and densification occurs [33, 34]. There may also be decomposition of crystalline compounds, formation of new phases and polymorphic transformations [34]. In this paper, in view of the points previously discussed, immobilized ZnO photocatalysts were produced by slip casting, through subsequent drying and sintering processes. The pellets were characterized, and their photocatalytic properties and reusability were evaluated.

EXPERIMENTAL

The slip casting process was used to obtain immobilized ZnO ceramic samples. The slurry was obtained with a mass composition of 70% ZnO (Synth) and 30% water [35]. The changes in viscosity due to the deflocculant variation in mass (Disperlan LA, Lamberti) were studied using a Brookfield viscometer (ADV). These analyzes were done with torque at 50%, rotation at 1.5 rpm, time at 2 min and spindle 64. All measurements were taken at 25 °C. The slip homogenization process was carried out using a high-energy SPEX SamplePrep 8000-series mill for 30 min. The ZnO/water/deflocculant mixture was added in a teflon flask, along with alumina beads, with a mass proportion of ball to slurry of approximately 30%. For the preparation of all ceramic samples (pellets), 28.0 g of ZnO and 12.0 g of water were used. Three different mixtures were made in which the deflocculant mass varied: 0.252 g (sample 1), 0.265 g (sample 2) and 0.276 g (sample 3). After the homogenization process, the slip was poured into plaster molds at 25 ºC. The drying time was 24 h. All the pieces were submitted to heat treatment in a muffle furnace (EDG, mod. 3000) in three stages. In the first step, the samples were heated to 100 °C at a rate of 3 °C/min and held at this temperature for 30 min to eliminate water. In the second step, they were heated to 800 °C at a rate of 10 °C/min for 10 h. Finally, in the third stage, they were cooled to 30 ºC at a rate of 1 ºC/min for 10 h.

Apparent porosity (AP) and apparent density (AD) tests were performed by the method based on the Archimedes Principle, using Eqs. A and B, respectively. For every weighing, an AY220 semi-analytical balance (Shimadzu) was used. For each sample, the dry mass (M_d) was determined. Subsequently, the samples were immersed in water at room temperature for 24 h. After this step, through an apparatus, the mass of each sample, still immersed in water (M_i), was determined. Finally, the excess water from the surface was removed with a damp cloth, obtaining the wet mass (M_w) for each sample.

$$AP = \frac{M_w - M_d}{M_w - M_i} 100 \quad (A)$$

$$AD = \frac{M_d}{M_w - M_i} d_{water} \quad (B)$$

To verify the crystalline structure of the samples, the X-ray diffraction (XRD) analyses were performed on a Shimadzu XRD6000 diffractometer using CuKα radiation (0.15456 nm) at 30 kV and 30 mA. The analyses were carried out with scanning at 2θ between 20° and 70°, an exposure time of 1 s and an angular pass of 0.021° in continuous mode. The particles morphologies were characterized by scanning electron microscopy (SEM, Jeol, JSM 6701F). For the photocatalytic assays, Rhodamine B (Synth) was used as a probe dye. Solutions containing 25 mL of Rhodamine B at a concentration of 5.0 $mg.L^{-1}$ along with a ZnO ceramic sample were prepared and irradiated for 120 min. The photocatalytic assays were performed in a batch reactor equipped with four Philips 15 W mercury lamps (UV-C, 254 nm). The dye concentration reduction was estimated based on color removal, which was determined by spectrophotometry (Cary 60 UV-vis, Agilent Technol.). Blank experiments were obtained by preparing Rhodamine

B solutions without ceramic samples (direct photolysis) and they showed no significant occurrence of dye degradation nor significant color removal in those conditions. Six cycles of photocatalysis were carried out for each sample.

RESULTS AND DISCUSSION

Fig. 1 shows the slurry viscosity curve as a function of the deflocculant concentration. A point where the curve shows an inflection can be observed. The main aim of this study was to verify if the viscosity had an influence on the final properties of the ceramic samples. In this way, the point of lowest inflection (6.58 g/g.10^{-3}) and the points closer to inflection, with concentrations of 6.26 g/g.10^{-3} and 6.85 g/g.10^{-3}, were chosen. It was also noted from the graph that a small change in the amount of deflocculant caused a significant change in the ZnO viscosity. From the three selected concentrations, ceramic samples were obtained and then submitted to heat treatment as described in the experimental procedure.

Table I shows the obtained results for apparent porosity and apparent density of the samples. The comparative differences in viscosities and density variations were not significant. The apparent density was, on average, 3.40±0.04 g/cm^3 and the apparent porosity was, on average, 40.2%±1.4%. These values indicated that the sample density results represented about 61% of the theoretical density of ZnO, which has a value of 5.61 g/cm^3. The X-ray diffractogram of the sample 1 is shown in Fig. 2. The sample presented the ZnO diffraction pattern with the wurtzite-type phase (JCPDS 36-1451). This was a positive factor because, according to the literature, this structure shows good photocatalytic activity [36-38]. No other crystalline phases were observed. The dimensions, morphology, and grain size

Table I - Apparent porosity and apparent density of the samples.

Sample	Apparent porosity (%)	Apparent density (g/cm^3)
1	41.34	3.40
2	38.64	3.44
3	40.75	3.36

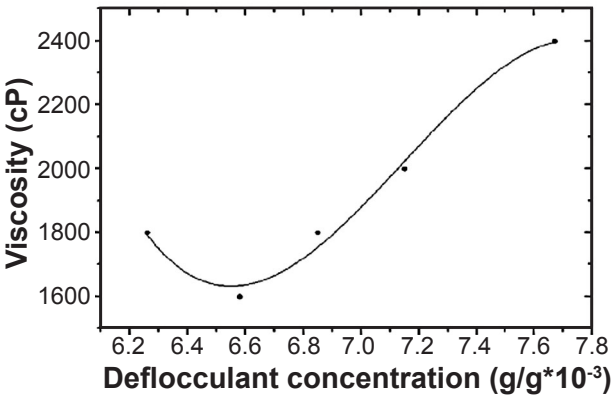

Figure 1: Graph of viscosity versus mass concentration of deflocculant.

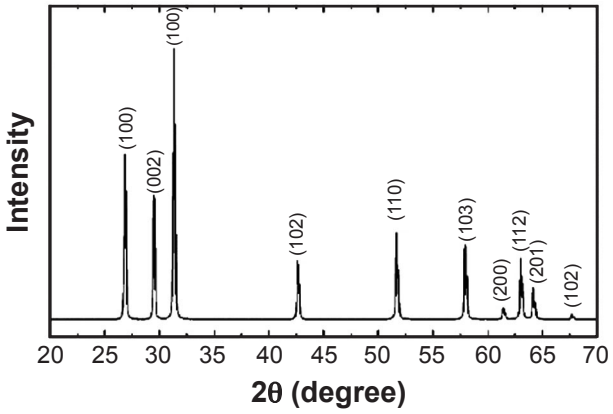

Figure 2: X-ray diffraction pattern of sample 1.

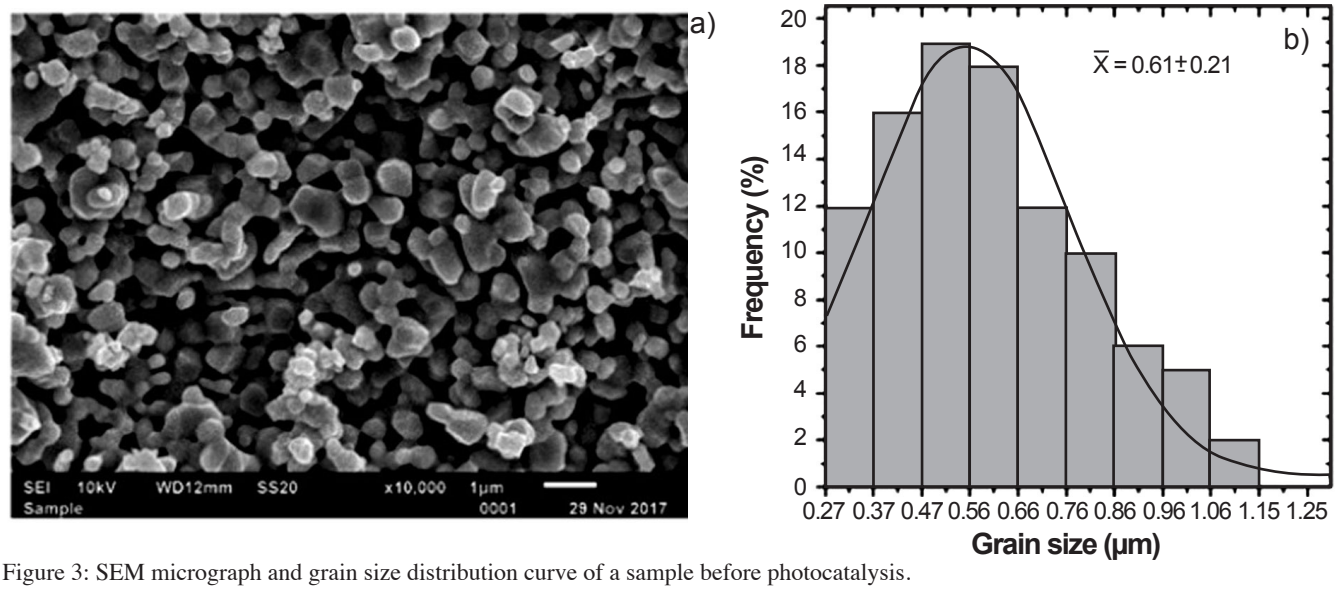

Figure 3: SEM micrograph and grain size distribution curve of a sample before photocatalysis.

distribution of a ZnO sample analyzed by SEM are shown in the image of Fig. 3. Such image shows mostly micrometric grain sizes, observed for all samples. The average grain size found for samples before photocatalysis was 0.61±0.21 μm, according to the histogram of grain size distribution presented in Fig. 3. The grains had an elongated shape, which indicated that during the heat treatment process necks were formed between the grains. The presence of pores in the sample was also verified. There are studies regarding ZnO films that obtained agglomerated irregular shaped columnar grains [39, 40], which are similar to those found in this study and typical of the hexagonal structure of the wurtzite phase, also found in this study's X-ray diffraction pattern (Fig. 2).

All samples were submitted to photocatalysis for an irradiation time of 120 min. The blank analysis corresponded to the analysis without the presence of the photocatalyst. The produced ZnO ceramic samples were used to photodegrade Rhodamine B under UV-C irradiation. An experiment with the same conditions was carried out in darkness to assess if the Rhodamine B adsorption could be neglected. Since no color removal was observed, the mentioned assumption was then confirmed. Fig. 4 shows the photocatalytic Rhodamine B degradation for ceramic samples obtained by three different viscosities and blank under UV-C irradiation. In all three different samples, color removal of the Rhodamine B solutions was observed. The kinetic from this semiconductor samples are shown in Fig. 5. According to Fig. 4, sample 1 presented 74% of Rhodamine B degradation, sample 2 77% and sample 3 81% within 120 min. Eq. C correlates the degradation time and the dye concentration assuming a pseudo-first order kinetics [41], where v is the reaction rate, [RhB] is the dye concentration, [AS] is the concentration of active sites, assumed as the total amount of independent points on the catalyst surface where the reaction takes place, and k is the velocity constant. This model has been applied satisfactorily in studies that address the degradation of Rhodamine B by photocatalysis [42, 43]:

$$v = -\frac{d[RhB]}{dt} k[RhB][AS] \quad (C)$$

The active sites concentration can be considered constant in all experiments, since they were in a steady state, which means that all dynamic events, such as recombination, were also in a steady state. In addition, as the light source was constant, the average number of active sites should be proportional to the surface area, which was the only variable that would directly affect the concentration of active sites under the given conditions. Being [AS] constant during a specific experiment, it can be coupled into a new constant k', shown in Eq. D. It is important to emphasize that the surface area is related to interferences in the total number of active sites for the formation of radicals on the surface of the photocatalysts and in the heterogeneous interaction between light, water, molecular oxygen and dye at the oxide surface [44]. Since the Rhodamine B color removal was monitored in relation to time, it was possible to obtain the reaction constant and the half-life time of each process under study.

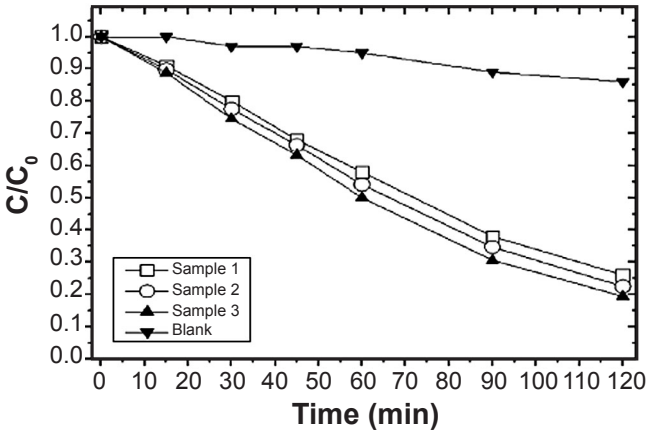

Figure 4: Concentration of Rhodamine B in relation to the irradiation time for the first cycle of ZnO ceramic samples.

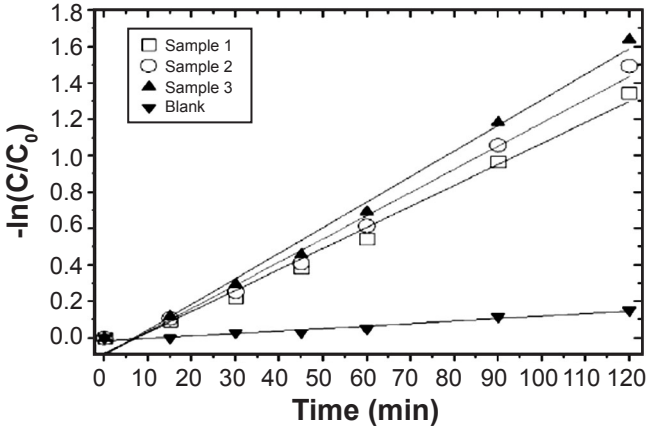

Figure 5: First order kinetics of Rhodamine B degradation for the first cycle of ZnO ceramic samples.

Eq. D shows the relation between the degradation time and the dye concentration, where k'=k.[AS], in which k is the velocity constant of the reaction, [AS] is the concentration of active sites on the catalyst surface, t is the irradiation time, and C represents the concentration of dye [45]:

$$-\ln\left(\frac{C}{C_0}\right) = k'.t \quad (D)$$

Eq. E was used to calculate the time required to reduce the concentration of organic compounds by half, where $t_{1/2}$ is the half-life time [45]:

$$t_{\frac{1}{2}} = \frac{\ln 2}{k'} \quad (E)$$

According to Eq. D, the graph obtained with $-\ln(C/C_0)$ versus t has an angular coefficient equal to the velocity constant of the reaction, k' [45]. Fig. 5 shows a graphical representation of this relation, in which a first-order kinetics was identified for all samples in all cycles of degradation. This pattern suggested that the same mechanism was activated in all degradations. The values of k' obtained, as well as the respective half-life times, for each sample of Figs. 4 and 5 can be observed in Table II, for the first cycle. These values were calculated using Eqs. D and E, respectively. For all

samples shown in Table II, the values of k' and $t_{1/2}$ obtained were close, with a maximum difference of 10 min. This indicated that all pellets produced, regardless of deflocculant concentration, were equally effective in the degradation of Rhodamine B, exhibiting similar rates of photodegradation and similar half-life times.

Table II - Values of k', R^2, and $t_{1/2}$ of the ceramic samples under irradiation (first cycle).

Sample	k' (min^{-1})	R^2	$t_{1/2}$ (min)
1	0.01152	0.985	60.17
2	0.01272	0.985	54.49
3	0.01402	0.988	49.44

In order to investigate the reuse capacity of the obtained ceramic samples, they were submitted to six cycles of photocatalysis. Fig. 6 shows the Rhodamine B degradation percentage of samples 1, 2 and 3 for all six cycles with 120 min/cycle. The degradation percentages presented in Fig. 6 show that there was a trend of degradation increase in the first three cycles for all the ceramic samples. It is also possible to observe that in the last three cycles, although the tendency was not maintained, the effectiveness of all the pieces remained, presenting high percentages of degradation in all cycles. All samples were reusable. The degradation percentage of sample 2 are shown both in Fig. 6b and Table III. Values of k', R^2 and $t_{1/2}$ are also shown in Table III. In the first three cycles, an increase in the photocatalytic efficiency of the ceramic samples was observed. The decrease in half-life time for these first three cycles of sample 2 corroborated this observation (Table III). This is believed to have occurred due to surface leaching during the first cycles of degradation. To investigate these results, scanning electron microscopy was performed after photocatalysis. The dimensions, morphology, and grain size distribution of a ZnO sample after photocatalysis analyzed by SEM are shown in Fig. 7. In comparison to Fig. 3 (sample before photocatalysis), Fig. 7 (sample after photocatalysis) presents smaller grains, of approximately 0.36±0.16 μm. In fact, according to the grain size distribution, a shift to regions of smaller grain size was observed. This indicated that larger grains, found on the surface of the pellets, were leached. It is worth mentioning

Table III - Values of k', R^2, and $t_{1/2}$ of the ceramic sample 2 under irradiation.

Cycle	k' (min^{-1})	R^2	$t_{1/2}$ (min)	Degradation (%)
1	0.01272	0.985	54.49	76.95
2	0.01854	0.964	37.39	89.22
3	0.02517	0.967	27.54	99.95
4	0.01736	0.975	39.93	87.10
5	0.02061	0.969	33.63	99.91
6	0.02579	0.988	26.88	99.95

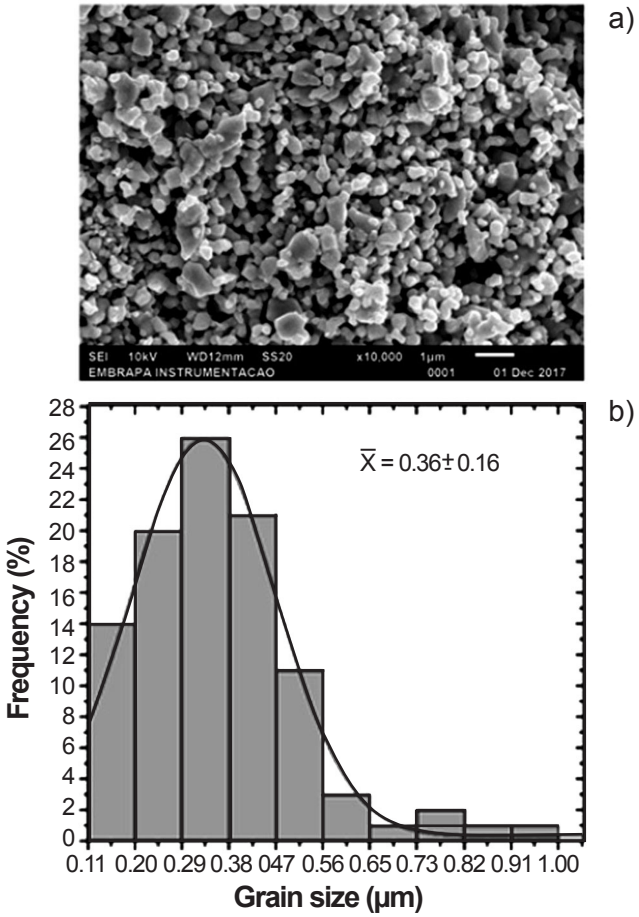

Figure 7: SEM micrograph and grain size distribution curve of a sample after photocatalysis.

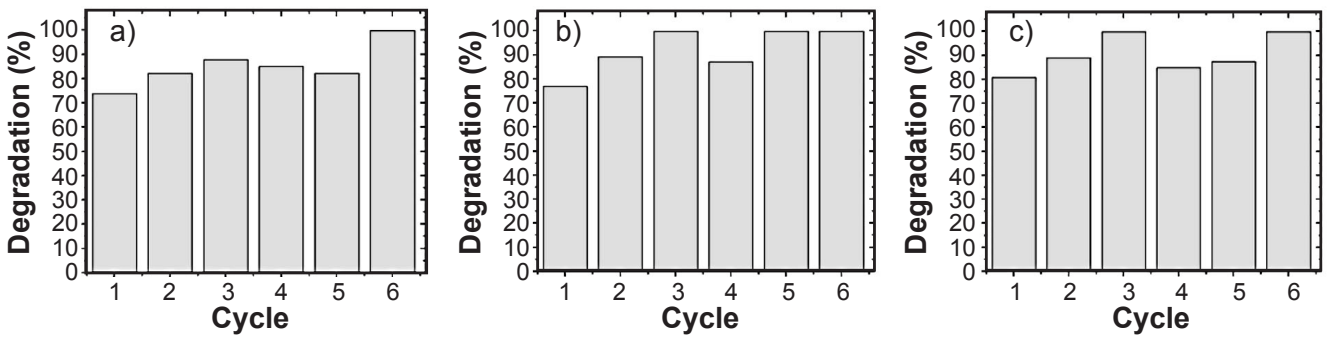

Figure 6: Graphical representations of dye degradation percentage versus number of cycles for samples: a) 1; b) 2; and c) 3.

that the difference between grain sizes (smaller inside the pellet and larger on the surface of the pellet) is known as abnormal grain growth and the main cause is probably related to the density inhomogeneity originated from the friction between the mold wall and the ZnO powders in the forming process [46, 47]. Due to this difference in morphology before and after the photocatalytic process, it can be inferred that surface leaching of the samples occurred during the cycles, which justified the improvement in the photocatalytic efficiency in the first three cycles. However, after the third cycle (Fig. 6), the efficiency was maintained. Thus, the reuse was not only favorable, but highly positive, since the analyzed ceramic ZnO samples presented a high potential for degrading Rhodamine B in several degradation cycles.

CONCLUSIONS

It was possible to obtain porous ZnO pellets by slip casting and partial sintering. The samples presented the wurtzite phase, with density and porosity of approximately 3.40±0.04 g/cm^3 and 40.2%±1.4%, respectively. The variation in the slurry viscosities had no influence on the final properties of the samples, both in degradation percentage and kinetics. The ZnO samples were satisfactorily applied in six cycles of photocatalysis and degraded around 89% of the Rhodamine B dye. The samples reuse is possible and desired, since the Rhodamine B degradation percentage increased with the increase of the number of cycles, possibly due to surface leaching.

ACKNOWLEDGMENTS

The authors gratefully acknowledge the Brazilian research funding programs and agencies CNPq (proc. 444117/2014-8), CAPES, and FAPEMIG (proc. APQ-01898-13) for their financial support. We are also grateful to the Federal University of Alfenas and Embrapa Instrumentação Agropecuária (SEG 01.14.03.001.01.00), São Carlos.

REFERENCES

[1] B. Kraeutler, A.J. Bard, J. Am. Chem. Soc. **100**, 19 (1978) 5985.
[2] H. Frischherz, F. Ollram, F. Scholler, E. Schmidt, Water Supply **4** (1986) 167.
[3] T. Kudo, Y. Nakamura, A. Ruike, Res. Chem. Intermed. **29** (2003) 631.
[4] D. Bahnemann, Sol. Energy **77** (2004) 445.
[5] O. Carp, C.L. Huisman, A. Reller, Prog. Solid State Chem. **32** (2004) 33.
[6] A. Kay, M. Grätzel, J. Phys. Chem. **97** (1993) 6272.
[7] B.A. Gregg, MRS Bull. **30** (2005) 20.
[8] E. Brillas, C.A. Martínez-Huitle, Appl. Catal. B **166** (2015) 603.
[9] A. Bes-Piá, J.A. Mendoza-Roca, M.I. Alcaina-Miranda, A. Iborra-Clar, M.I. Iborra-Clar, Desalination **149** (2002) 169.
[10] M.A. Henderson, Surf. Sci. Rep. **66** (2011) 185.
[11] M. Panizza, G. Cerisola, J. Hazard. Mater. **153** (2007) 83.
[12] C.A. Martínez-Huitle, S. Ferro, Chem. Soc. Rev. **35**, 12 (2006) 1324.
[13] S.E. Braslavsky, Pure Appl. Chem. **79**, 3 (2007) 293.
[14] S.A. Ansari, M.M. Khan, M.O. Ansari, J. Lee, M.H. Cho, J. Phys. Chem. C **117** (2013) 27023.
[15] S.S. Borges, L.P.S. Xavier, A.C. Silva, S.F. Aquino, Quim. Nova **39** (2016) 836.
[16] I.M. Arabatzis, S. Antonaraki, T. Stergiopoulos, A. Hiskia, E. Papaconstantinou, M.C. Bernard, P. Falaras, J. Photochem. Photobiol. A **149** (2002) 237.
[17] I. Mazzarino, P. Piccinini, L. Spinelli, Catal. Today **48** (1999) 315.
[18] M.P.F. Graça, C.C. Silva, L.C. Costa, M.A. Valente, Int. J. Nanoelec. Mater. **3** (2010) 99.
[19] J. Yang, B. Wei, X. Li, J. Wang, H. Zhai, X. Li, Y. Sui, Y. Li, J. Wang, J. Lang, Q. Zhang, Cryst. Res. Technol. **50**, 11 (2015) 840.
[20] P. Jongnavakit, P. Amornpitoksuk, S. Suwanboon, T. Ratana, Thin Solid Films **520** (2012) 5561.
[21] T. Wanotayan, J. Panpranot, J. Qin, Y. Boonyongmaneerat, Mat. Sci. Semicon. Proc. **74** (2018) 232.
[22] B. Pal, M. Sharon, Mater. Chem. Phys. **76** (2002) 82.
[23] R. Moreno, Am. Ceram. Soc. **71**, 10 (1992) 1521.
[24] Y.N. Kryuchkov, T.L. Neklyudova, Glass Ceram. **71**, 9 (2015) 324.
[25] J.M.F. Ferreira, S.M. Olhero, Ceram. Int. **28** (2002) 377.
[26] P. Reynaud, M. Saâdaouni, S. Meille, G. Fantozzi, J. Eur. Ceram. Soc. **23** (2003) 3105.
[27] P. Reynaud, M. Saâdaouni, S. Meille, G. Fantozzi, J. Eur. Ceram. Soc. **25** (2005) 3281.
[28] C.M.F. Vieira, H.S. Feitosa, S.N. Monteiro, Ceram. Ind. **8**, 1 (2003) 42.
[29] J.J.S. Nascimento, A.G.B. Lima, B.J. Teruel, F.A. Belo, Inf. Tecnol. **17**, 6 (2006) 145.
[30] G. Musielak, Dry. Technol. **19**, 8 (2001) 1645.
[31] R. Maciulaitis, J. Malaiškien, J. Civil Eng. Manag. **15**, 2 (2009) 197.
[32] G. Musielak, D. Mierzwa, Dry. Technol. **27**, 7-8 (2009) 894.
[33] M.N. Rahaman, *Ceramic processing and sintering*, CRC Press, New York (2003).
[34] W.D. Kingery, H.K. Bowen, D.R. Uhlmann, *Introduction to ceramics*, Wiley-Intersci., Massachusetts (1976).
[35] J.C. Junior, "Desenvolvimento de uma massa cerâmica para produção de peças especiais esmaltadas para revestimento através do método de colagem", Diss. Mestr., Un. Fed. Santa Catarina (2004).
[36] R.G. Carvalho, M.T.S. Tavares, F.K.F. Oliveira, R.M. Nascimento, E. Longo, M.S. Li, C.A. Paskocimas, M.R.D. Bomio, F.V. Motta, J. Mater. Sci. **28** (2017) 7943.
[37] A.L.M. Oliveira, J.M. Ferreira, M.R.S. Silva, S.C. Souza, F.T.G. Vieira, E. Longo, J. Therm. Anal. Calorim. **97**

(2009) 167.
[38] D.A. Vieira, V.V.S. Diniz, R.H.G.A. Kiminami, D.R. Cornejo, V.E. Lima, A.C.F.M. Costa, Rev. Virt. Quím. **8** (2016) 1817.
[39] J. Yang, S. Na, W. Park, G. Yi, W. Choi, Adv. Mater. **16** (2004) 1661.
[40] R. Uma, K. Ravichandran, Kinet. Catal. **58**, 6 (2017) 701.
[41] H.S. Fogler, *Elements of chemical reaction engineering*, Pergamon, Massachusetts (1987).
[42] J.A. Oliveira, A.E. Nogueira, M.C.P. Gonçalves, E.C. Paris, C. Ribeiro, G.Y. Poirier, T.R. Giraldi, Appl. Surf. Sci. **433** (2018) 879.
[43] V.R. de Mendonça, C. Ribeiro, Appl. Catal. B **105** (2011) 298.
[44] Y.V. Kolen'ko, B.R. Churagulov, M. Knust, L. Mazerolles, C. Colbeau-Justin, Appl. Catal. B **54** (2004) 51.
[45] Q.I. Rahman, M. Ahmad, S.K. Misra, M. Lohani. Mater. Lett. **91** (2013) 170.
[46] H.M. Macleod, K. Marshall, Powder Technol. **16**, 1 (1997) 107.
[47] B.J. Briscoe, S.L. Rough. Colloids Surf. A **137** (1997) 103.
(Rec. 31/08/2018, Rev. 08/11/2018, Ac. 11/11/2018)